Optical Materials 41 (2015) 36–40

Contents lists available at ScienceDirect

Optical Materials

journal homepage: www.elsevier.com/locate/optmat

Optical and scintillation properties of Nd differently doped $YLiF_4$ from VUV to NIR wavelengths

Takayuki Yanagida [a,*], Yutaka Fujimoto [a], Sumito Ishizu [b], Kentaro Fukuda [b]

[a] Kyushu Institute of Technology, 2-4 Hibikino, Wakamatsu-ku, Kitakyushu 808-0196, Japan
[b] Tokuyama Corp., 1-1 Mikage-cho, Shunan-shi, Yamaguchi 745-8648, Japan

ARTICLE INFO

Article history:
Available online 6 November 2014

Keywords:
Crystal
Scintillation detector
Nd^{3+}
Scintillator

ABSTRACT

Nd 0.1, 0.5, 1, and 3 mol% doped $YLiF_4$ crystalline scintillators were prepared by Tokuyama Corp. and their optical and scintillation properties from vacuum ultraviolet (VUV) to near infrared (NIR) wavelengths were investigated. 4f–5d absorption bands appeared in VUV and several absorption bands due to 4f–4f transition were observed in visible-NIR wavelengths. Nd^{3+} 5d–4f emission was observed around 180 nm under 160 nm excitation and intense line due to $^4F_{3/2} \rightarrow {}^4I_{11/2}$ at 1064 nm appeared under 500 nm excitation. In X-ray induced radioluminescence, both VUV and NIR emissions were observed. Scintillation decay times of VUV emission was 40–80 ns while that of 4f–4f ones at visible wavelength were around 12–15 μs. When ^{252}Cf neutron was irradiated, VUV scintillation light yield resulted around 90 ph/n.

1. Introduction

Scintillators are one of the luminescent materials which convert high energy ionizing radiation to thousands of low energy photons immediately. Spectrum of practical applications are wide including medical [1], security [2], well-logging [3], astrophysics [4], and particle physics [5]. In such applications, scintillators with visible emission are preferable because the wavelength sensitivity of one of the conventional photodetectors, photomultiplier tube (PMT), is high at visible wavelength. However, recent progress of novel photodetectors opens a new possibility to use scintillators with other emission wavelengths. If efficient vacuum ultra violet (VUV) emitting scintillators are found, we can use a gas proportional counter as photodetectors (gas-PMT). The idea of gas-PMT was raised around 90's [6,7] and recently some new types of gas-PMT were investigated [8,9]. On the other hand, near infrared (NIR) scintillation attracted some attentions due to its high penetration power to human body [10]. In bio imaging, NIR emission with persistent luminescence can be considered as kinds of marker in human body [11]. Historically, NIR emitting scintillators were studied around 2000 [12,13] and no follow-up research was not done. Recently, we re-started NIR emitting scintillator for a real time monitor in radiation therapy and examined Nd, Ho, Er, and Tm-doped garnet crystals at first [14]. Therefore VUV ($\lambda < 200$ nm) and NIR ($\lambda > 650$ nm) scintillation are interesting for future applications.

To our knowledge, previous studies about VUV or NIR emitting scintillators concentrated on their focusing wavelengths and there were no investigations on a relation of VUV and NIR scintillation in one material system. A simple question, which emission is dominant, VUV or NIR, cannot be answered in experimental viewpoints. Though one thinks it is obvious by concerning photon energies of VUV (>6 eV) and NIR (<2 eV), experimental evidences are important. To investigate such a basic point, we studied Nd^{3+} differently doped $YLiF_4$ crystals on optical and scintillation characteristics because VUV scintillation of trivalent rare earth ions could be observed in widegap materials and we could not observe it in conventional (e.g., oxide) materials. Nd-doped $YLiF_4$ is famous in laser applications [15] and is known to exhibit VUV emission due to Nd^{3+} 5d–4f transition [16–18].

In this work, Nd 0.1, 0.5, 1, and 3 mol% doped $YLiF_4$ crystalline scintillators were prepared by Tokuyama Corp. with micro-pulling down technique. In these four samples, optical and scintillation properties were investigated. In addition, thermally stimulated luminescence (TSL) glow curves and X-ray induced afterglow (= TSL around room temperature) were studied to investigate the effect of the dopant concentration.

2. Experimental

Crystal growth was performed in a vacuum-tight micro-pulling down system equipped with radio frequency induction heater. Commercially available fluoride powders of LiF, YF_3 and NdF_3 (>99.99%) were mixed and charged into a crucible made of high

* Corresponding author. Tel./fax: +81 93 695 6049.
E-mail address: yanagida@lsse.kyutech.ac.jp (T. Yanagida).

http://dx.doi.org/10.1016/j.optmat.2014.10.043
0925-3467/

purity graphite with a 2 mm diameter hole at the bottom. The concentrations of NdF_3 in the starting material were 0.1, 0.5, 1, and 3 mol%. The reason to choose these concentrations is like this. Generally, 0.5–1 mol% doping concentration is optimum for scintillators and we also prepared high (3 mol%) and low (0.1 mol%) dopant concentrations for comparison. The starting materials were treated by heating under vacuum to eliminate water traces prior to crystal growth. Subsequently, high-purity CF_4/Ar gas was introduced into the furnace and the starting materials were melted. Nd doped $YLiF_4$ crystals were pulled down at growth rate of 3 mm/h from the hole of crucible. The initial part of grown crystals were cut and polished into 2×7–$10 \times 1\ mm^3$ for the evaluation of optical and scintillation properties.

In-line transmittances of all samples were evaluated by using JASCO V670 spectrometer from 190 to 2700 nm and by our original system [19] from 120 to 300 nm, respectively. Photoluminescence (PL) from 100 to 700 nm under 160 nm excitation was evaluated by the original setup [19] and from 650 to 1650 nm under 500 nm excitation by Andor DU-420-BU2 CCD spectrometer. In VUV, there was no available data of the quantum efficiency of CCD and we could not discuss the emission intensity. In X-ray induced radioluminescence, the X-ray generator was used as an excitation source and detectors were same with those in PL measurements. Two detectors had an overlap wavelength at 650–700 nm and we used this range to connect spectral data. In this overlap range, spectral sensitivity of the original set up was around 25% taking into account the quantum efficiency of CCD (~50%) and the grating (~50%). On the other hand, that of NIR spectrometer was 0.5% due to a low quantum efficiency of the InGaAs CCD (~10%) and the grating (~5%). In NIR at wavelength longer than 900 nm, the sensitivity against the wavelength was almost flat. The quantum efficiency of InGaAs CCD was around 80% and the efficiency of the grating was 60%. It should be noted that presented spectra were not spectrally corrected. Scintillation decay time profiles were recorded by our recent developed system [20] which enabled us to evaluate scintillation from 160 to 650 nm without wavelength resolution. By using VUV optical filter (ACTON, 180-N-1D), 5d–4f and 4f–4f scintillations were distinguished.

In order to evaluate scintillation light yield, ^{252}Cf irradiated pulse height spectra were evaluated since $YLiF_4$ contained Li in the chemical composition and was potentially applicable for neutron scintillation detectors based on $^6Li(n,\alpha)^3H$ nuclear reaction. The samples were wrapped with several layers of Teflon tape to collect scintillation photons and were coupled to PMT R8778 (Hamamatsu) with Krytox (Dupont, a VUV transparent grease). This PMT was specially designed to detect scintillation photons from liquid Xe (172 nm emission wavelength) in XMASS project [21]. The high voltage of −1300 V was supplied by ORTEC 556 power unit, and the signal was then read out from the anode of the PMT. Thereafter, the signals were fed into a preamplifier ORTEC 113 and shaping amplifier ORTEC 570 with 0.5 μs shaping time. After being converted to digital signals by a multi channel analyzer Pocket MCA 8000A provided by Amptek Co., they were recorded on a computer. At present, we cannot evaluate NIR scintillation light yield quantitatively since general shaping times (few to 10 μs) is too short to accumulate NIR photons. In addition, huge dark current of NIR sensitive PMTs and wavelength limitation up to 1000 nm in general Si photodiodes including avalanche-type are also problems to evaluated NIR scintillation. To grasp a change of trap sites by Nd concentrations, TSL glow curves were evaluated by Nanogray TL2000 [22] after 1 Gy X-ray exposure. X-ray induced afterglow was also evaluated by using the same set up with scintillation decay time and the X-ray exposure time was 2 ms.

3. Results and discussion

Fig. 1 demonstrates cut and polished samples. As shown in the figure, all samples were visibly transparent and they had a size of $2 \times 1 \times 7$–$10\ mm^3$. The wide surface areas were used for optical and scintillation characteristics.

Fig. 2 represents in-line transmittance spectra of Nd-doped $YLiF_4$ crystals in VUV (a) and the other (b) wavelengths. All sample showed a deep absorption below 175 nm due to Nd^{3+} 4f–5d transition and VUV absorption features resembled with those of Nd-doped $LuLiF_4$ [23] since they had a same crystal structure. Nd 0.1% doped sample exhibited worse transmittance of 50–60% at wavelength longer than 200 nm. We experienced similar phenomenon in Ce-doped $LuLiF_4$. Ce 0.1% dope $LuLiF_4$ had a difficulty in crystal growth and showed worse transmittance than Ce 0.5% and 1% doped samples [24]. Crystal growth of $YLiF_4$ or $LuLiF_4$ with small rare earth doping concentrations may be difficult in our experimental condition.

Fig. 3 demonstrates PL spectra under 160 nm excitation in 100–700 nm (a) and under 500 nm excitation in 650–1650 nm (b), respectively. In VUV wavelength, emission lines at 180 ($5d_1 \rightarrow {}^4I_{9/2}$), 230 ($5d_1 \rightarrow {}^4F_i$), and 260 ($5d_1 \rightarrow {}^2H_i$) nm were observed. On the other hand in NIR wavelength, intense emission bands appeared around 900, 1064, and 1315 nm and these bands were ascribed to the transition from Nd^{3+} $^4F_{3/2}$ excited states to $^4I_{9/2}$, $^4I_{11/2}$, and $^4I_{13/2}$, respectively. These emission lines were typical in 4f–4f transition of Nd^{3+} ion. Though emission intensities of 5d–4f luminescence were similar in all samples, $^4F_{3/2} \rightarrow {}^4I_{11/2}$ line (1064 nm) of Nd 0.1% doped sample was weaker than the other samples.

X-ray induced radioluminescence spectra from VUV to NIR wavelengths are shown in Fig. 4. In VUV wavelength, 180 nm emission due to Nd^{3+} $5d_1 \rightarrow {}^4I_{9/2}$ transition was the dominant peak in all samples and emission intensities of them were similar levels. Observed spectra resembled to those of Nd-doped $LuLiF_4$ [23]. In NIR wavelength, Nd^{3+} $^4F_{3/2} \rightarrow {}^4I_{11/2}$ transition around 1064 nm was a dominant one and it was a famous line for laser applications. Spectral feature of NIR wavelength was similar to that of Nd-doped $LuLiF_4$ under α-ray excitation [25]. Unlike PL spectra, emission bands around 540 and 600 nm appeared and these bands were ascribed to $^4I_{9/2} \rightarrow ({}^2G_{9/2}, {}^4G_{11/2}, {}^2K_{15/2}, {}^2D_{3/2})$ and $^4I_{9/2} \rightarrow ({}^4G_{5/2}, {}^2G_{7/2})$ transitions, respectively.

Fig. 5 demonstrates X-ray induced scintillation decay time profiles of Nd^{3+}-doped $YLiF_4$. In VUV scintillation selected by VUV optical filter, fast spike like component and relatively slow component were detected (Fig. 5(a)). The former one was 1–2 ns exponential decay and would be due to an instrumental artifact, an accidental thermal noise or X-ray direct hit to PMT photocathode since the timing response of used PMT (R7400P) was around 1 ns. This interpretation was supported by the excitation pulse also plotted in this figure. Relatively slow component was due to Nd^{3+} 5d–4f transition. Decay time constants of Nd 0.1, 0.5, 1, and 3 mol% doped samples resulted 98, 54, 44, and 38 ns, respectively. Compared with other Nd-doped VUV emitting scintillators, observed values were relatively slower. Previously, 30 ns under two-photon excitation

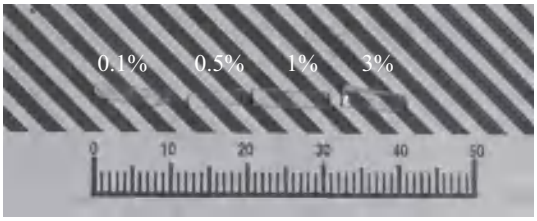

Fig. 1. Photograph of Nd-doped $YLiF_4$ crystals.

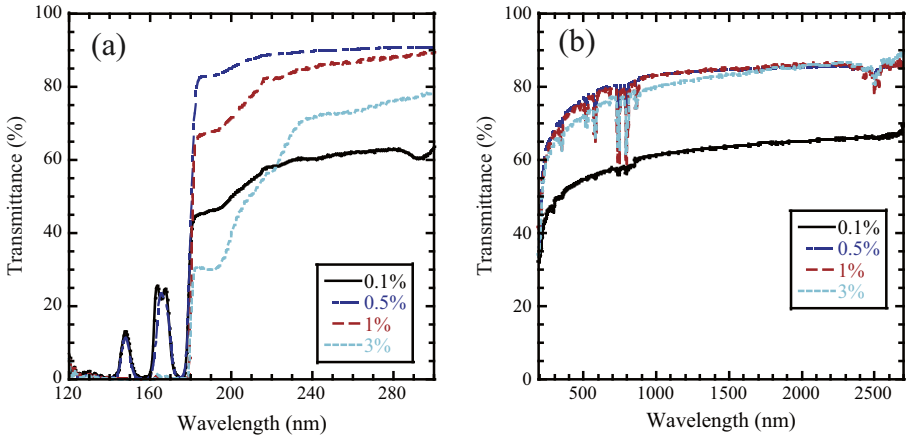

Fig. 2. In-line transmittance spectra in 120–300 nm (a) and 190–2700 nm (b).

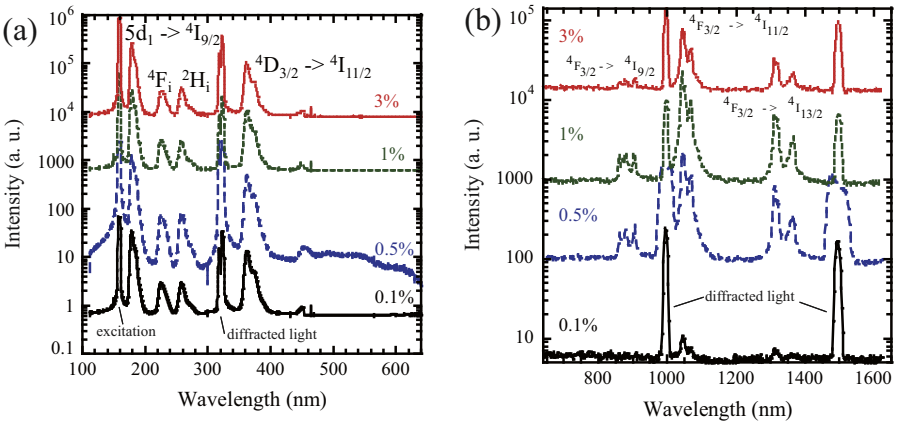

Fig. 3. PL spectra in 100–700 nm under 160 nm excitation (a) and 650–1650 nm under 500 nm excitation (b). Data are not corrected spectrally.

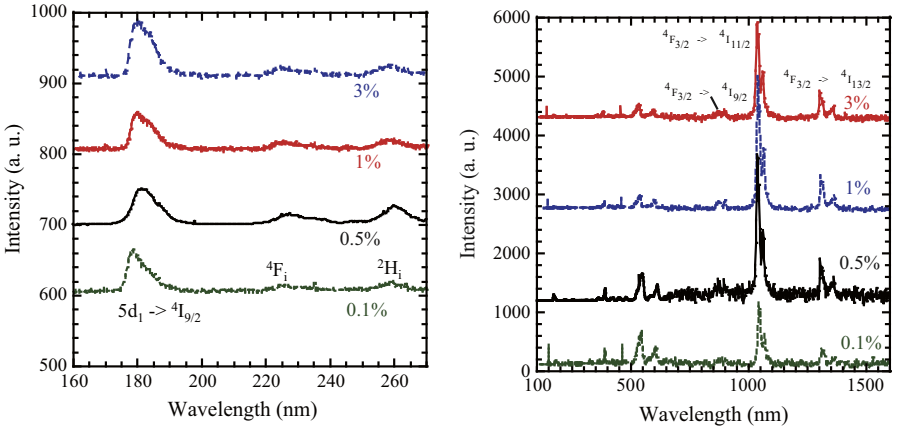

Fig. 4. X-ray induced radioluminescence spectra in 100–700 nm (a) and 650–1650 nm (b). Data are not corrected spectrally.

[16], 23 ns under VUV (7.8 eV) excitation [17] and 50–60 ns (rough estimation from the graph [17] by eyes) under soft-X-ray (30 eV) decay times were reported in Nd-doped $YLiF_4$. It was a general phenomenon that scintillation was slower than PL due to an additional energy migration process from the host to emission centers. In view of the scintillation, the soft-X-ray result observed in Nd 1.5% doped sample [17] and our results were similar. Our 1% sample was faster than previous 1.5% sample [17] and it would be blamed for the difference of actual Nd concentration since it was a common sense that the actual doping concentration depended on the manufacturing processes. Therefore in $YLiF_4$ host, Nd^{3+} 5d–4f transition was slower than other Nd^{3+}-doped VUV emitting scintillators. On the other hand, 4f–4f transitions were characterized by 12–15 μs decay time (Fig. 5(b)). In this figure, we also plotted the excitation pulse and it was apparently negligible for the analysis. Thus at least in visible wavelength, Nd^{3+} 4f–4f emission was acceptable as scintillator since $CdWO_4$ which was one of the conventional scintillators exhibited similar time response. Both

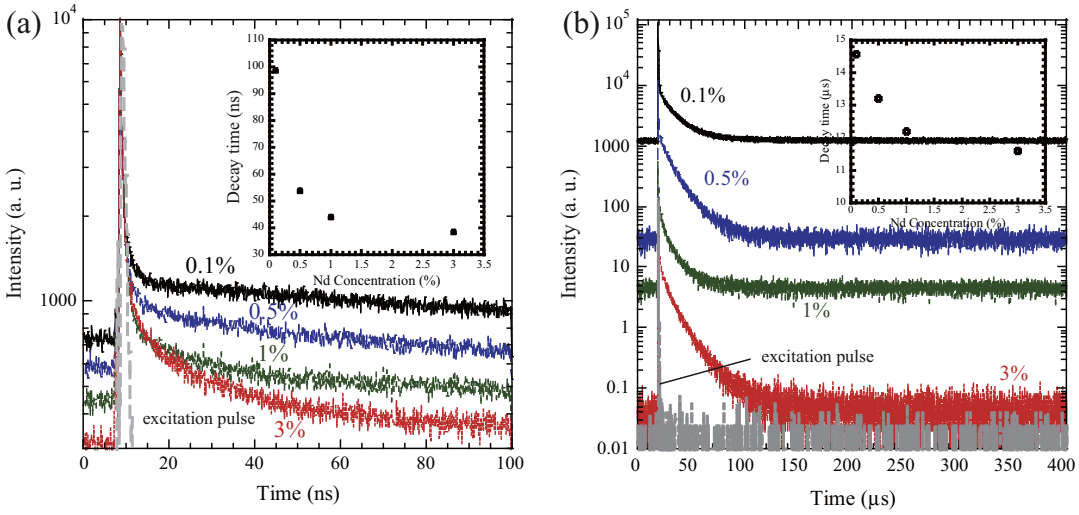

Fig. 5. Scintillation decay time profiles of Nd^{3+} 5d–4f (a) and 4f–4f transitions. Inset shows the relation between the decay time and Nd concentrations. The excitation pulse is also plotted in the figure.

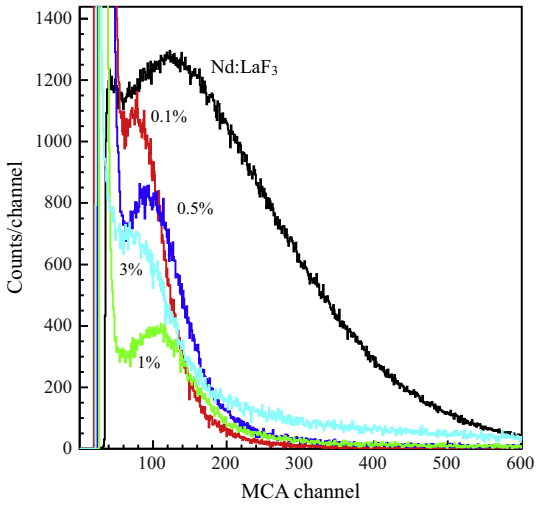

Fig. 6. ^{252}Cf neutron irradiated pulse height spectra of Nd-doped $YLiF_4$ compared with Nd-doped LaF_3 under ^{241}Am α-ray excitation.

5d–4f and 4f–4f decay times became faster when Nd doping concentration was increased.

^{252}Cf irradiated pulse height spectra of present samples compared with Nd-doped LaF_3 under ^{241}Am α-ray irradiation are shown in Fig. 6. The standard Nd-doped LaF_3 had a scintillation light yield of ~100 ph/5.5 MeV-α under the evaluation using the same size sample prepared by the same manufacturer [9] and had similar scintillation wavelength with Nd-doped $YLiF_4$. As a result, Nd 1 mol% doped sample exhibited the highest light yield and the value was ~90 ph/n. It was consistent with radioluminescence that all sample showed light yields with similar levels.

In Fig. 7, TSL glow curves after 1 Gy X-ray exposure are depicted. TSL intensity was the strongest in Nd 0.1% doped sample and the glow peak appeared around 190 °C. When the doping concentration increased, 190 °C peak disappeared and new peaks around 250 °C and 350 °C were generated. The origin of 190 °C peak would be $YLiF_4$ host and new trap sites would be created by an introduction of Nd^{3+} ion into the host lattice. Then, X-ray induced afterglow time profiles of Nd-doped $YLiF_4$ are illustrated in Fig. 8. Afterglow is TSL around room temperature and one of the most important properties for X-ray CT and security systems in airports. Observed results were consistent with TSL glow curves. The highest TSL sample, Nd 0.1% doped $YLiF_4$ showed the worst afterglow level and remaining three samples resulted similar levels. Compared with other conventional scintillators for X-ray CT or security systems [20], observed afterglow levels worse in two digits.

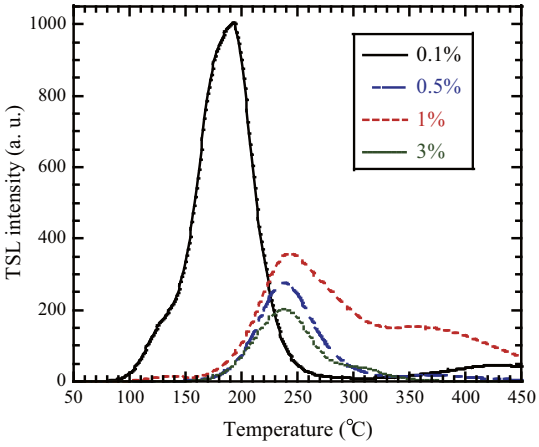

Fig. 7. TSL glow curves of Nd-doped $YLiF_4$ scintillators after 1 Gy X-ray exposure.

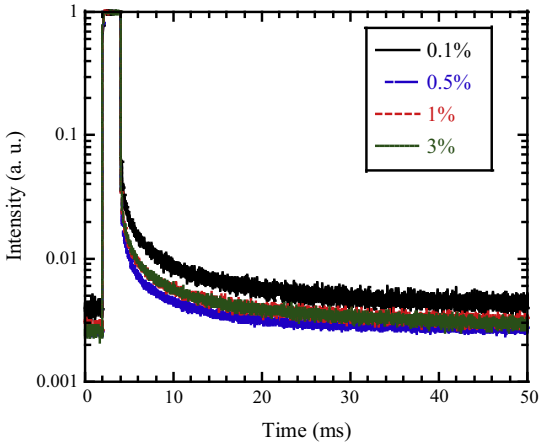

Fig. 8. X-ray induced afterglow time profiles of Nd-doped $YLiF_4$ scintillators.

4. Conclusion

Nd^{3+} 0.1, 0.5, 1, and 3 mol% doped $YLiF_4$ crystals were synthesized by Tokuyama Corp. and evaluated on their optical and scintillation properties from VUV to NIR wavelengths. In scintillation, VUV emission around 180 nm due to Nd^{3+} 5d–4f transition and NIR emission around 1064 nm due to Nd^{3+} $^4F_{3/2} \rightarrow {}^4I_{11/2}$ transition were observed. VUV scintillation light yield under ^{252}Cf neutron was around 90 ph/n. X-ray induced afterglow was evaluated and afterglow levels were worse than conventional scintillators for X-ray CT or security systems around two digits.

Acknowledgments

This work was mainly supported by a Grant in Aid for Scientific Research (A)-26249147 from the Ministry of Education, Culture, Sports, Science and Technology of the Japanese government (MEXT) and partially by JST A-step. Partial assistance from Nippon Sheet Glass Foundation for Materials Science and Engineering, Tokuyama Science foundation, Iketani Science and Technology Foundation, Hitachi Metals Materials Science Foundation, Mazda Foundation, JFE 21st century Foundation, and The Asahi Glass Foundation, the Cooperative Research Project of Research Institute of Electronics, Shizuoka University and Collaborative Research Program of Institute for Chemical Research, Kyoto University (2014-31) are also gratefully acknowledged.

References

[1] T. Yanagida, A. Yoshikawa, Y. Yokota, K. Kamada, Y. Usuki, S. Yamamoto, M. Miyake, M. Baba, K. Sasaki, M. Ito, IEEE Nucl. Trans. Sci. 57 (2010) 1492.
[2] D. Totsuka, T. Yanagida, K. Fukuda, N. Kawaguchi, Y. Fujimoto, Y. Yokota, A. Yoshikawa, Nucl. Instrum. Meth. A 659 (2011) 399.
[3] T. Yanagida, Y. Fujimoto, S. Kurosawa, K. Kamada, H. Takahashi, Y. Fukazawa, M. Nikl, V. Chani, Jpn. J. Appl. Phys. 52 (2013) 076401.
[4] K. Yamaoka, M. Ohno, Y. Terada, S. Hong, J. Kotoku, Y. Okada, A. Tsutsui, Y. Endo, K. Abe, Y. Fukazawa, S. Hirakuri, T. Hiruta, K. Itoh, T. Itoh, T. Kamae, M. Kawaharada, N. Kawano, K. Kawashima, T. Kishishita, T. Kitaguchi, M. Kokubun, G.M. Madejski, K. Makishima, T. Mitani, R. Miyawaki, T. Murakami, M.M. Murashima, K. Nakazawa, H. Niko, M. Nomachi, K. Oonuki, G. Sato, M. Suzuki, H. Takahashi, I. Takahashi, T. Takahashi, S. Takeda, K. Tamura, T. Tanaka, M. Tashiro, S. Watanabe, T. Yanagida, D. Yonetoku, IEEE Trans. Nucl. Sci. 52 (2005) 2765.
[5] T. Ito, M. Kokubun, T. Takashima, T. Yanagida, S. Hirakuri, R. Miyawaki, H. Takahashi, K. Makishima, T. Tanaka, K. Nakazawa, T. Takahashi, T. Honda, IEEE Trans. Nucl. Sci. 53 (2006) 2983.
[6] J. van der Marel, V.R. Born, C.W.E. van Eijk, R.W. Hollander, P.M. Sarrob, Nucl. Instrum. Meth. A 392 (1997) 310.
[7] P. Schotanus, C.W.E. Van Eijk, R.W. Hollander, Nucl. Instrum. Meth. A 272 (1988) 913.
[8] R. Chechik, A. Breskin, Nucl. Instrum. Meth. A 595 (2008) 116.
[9] H. Sekiya, C. Ida, H. Kubo, S. Kurosawa, K. Miuchi, T. Tanimori, K. Taniue, A. Yoshikawa, T. Yanagida, Y. Yokota, K. Fukuda, S. Ishizu, N. Kawaguchi, T. Suyama, Nucl. Instrum. Meth. A 633 (2011) S36.
[10] T. Yanagida, Y. Fujimoto, H. Yagi, T. Yanagitani, Opt. Mater. 36 (2014) 1044.
[11] C. Amiot, S. Xu, S. Liang, L. Pan, J. Zhao, Sensors 8 (2008) 3082.
[12] W.W. Moses, M.J. Weber, S.E. Derenzo, D. Perry, P. Berdahl, L.A. Boatner, IEEE Trans. Nucl. Sci. 45 (1998) 462.
[13] P.A. Rodnyi, E.I. Gorohova, S.B. Mikhrin, A.N. Mishin, A.S. Potapov, Nucl. Instrum. Meth. A 486 (2002) 244.
[14] T. Yanagida, Opt. Mater. 35 (2013) 1987.
[15] N.U. Wetter, Neodymium doped lithium yttrium fluoride (Nd:YLiF4) lasers, Handbook of Solid-State Lasers, 2013, pp. 323–340 (Chapter 12).
[16] P.W. Dooley, J. Thøgersen, J.D. Gill, H.K. Haugen, R.L. Brooks, Opt. Commun. 183 (2000) 451.
[17] A.N. Belsky, P. Chevallier, J.Y. Gesland, N.Yu. Kirikova, J.C. Krupa, V.N. Makhov, P. Martin, P.A. Orekhanov, M. Queffelec, J. Lumin. 72–74 (1997) 146.
[18] N.M. Khaidukov, M. Kirm, S.K. Lam, D. Lo, V.N. Makhov, G. Zimmerer, Opt. Commun. 184 (2000) 183.
[19] N. Abe, Y. Yokota, T. Yanagida, N. Kawaguti, M. Nikl, K. Fukuda, A. Yoshikawa, J. Pejchal, M. Nikl, IEEE Nucl. Trans. Sci. 57 (2010) 1278.
[20] T. Yanagida, Y. Fujimoto, T. Ito, K. Uchiyama, K. Mori, Appl. Phys. Exp. 7 (2014) 062401.
[21] S. Moriyama, Proceedings of the International Workshop on Technique and Application of Xenon Detectors, World Scientific 2002, 2002, 123.
[22] T. Yanagida, Y. Fujimoto, N. Kawaguchi, S. Yanagida, J. Ceram. Soc. Jpn. 121 (2013) 989.
[23] T. Yanagida, N. Kawaguchi, S. Ishizu, Y. Yokota, K. Fukuda, T. Suyama, A. Yoshikawa, H. Sekiya, S. Kubo, T. Tanimori, V. Chani, IEEE Trans. Nucl. Sci. 57 (2010) 1312.
[24] T. Yanagida, Y. Fujimoto, K. Fukuda, V. Chani, Nucl. Instrum. Meth. A 729 (2013) 58.
[25] A. Yamaji, Y. Fujimoto, T. Yanagida, N. Kawaguchi, K. Fukuda, Y. Yokota, A. Yoshikawa, Opt. Mater. 35 (2013) 1890.